

Folded Recurrent Neural Networks for Future Video Prediction

Marc Oliu

Universitat Oberta de Catalunya
Centre de Visió per Computador
Rambla del Poblenou, 156, 08018 Barcelona
moliu@uoc.edu

Javier Selva

Universitat de Barcelona
Gran Via de les Corts Catalanes, 585, 08007 Barcelona
javier.selva.castello@est.fib.upc.edu

Sergio Escalera

Universitat de Barcelona
Centre de Visió per Computador
Gran Via de les Corts Catalanes, 585, 08007 Barcelona
sergioescalera@cvc.uab.edu

Abstract

Future video prediction is an ill-posed Computer Vision problem that recently received much attention. Its main challenges are the high variability in video content, the propagation of errors through time, and the non-specificity of the future frames: given a sequence of past frames there is a continuous distribution of possible futures. This work introduces bijective Gated Recurrent Units, a double mapping between the input and output of a GRU layer. This allows for recurrent auto-encoders with state sharing between encoder and decoder, stratifying the sequence representation and helping to prevent capacity problems. We show how with this topology only the encoder or decoder needs to be applied for input encoding and prediction, respectively. This reduces the computational cost and avoids re-encoding the predictions when generating a sequence of frames, mitigating the propagation of errors. Furthermore, it is possible to remove layers from an already trained model, giving an insight to the role performed by each layer and making the model more explainable. We evaluate our approach on three video datasets, outperforming state of the art prediction results on MMNIST and UCF101, and obtaining competitive results on KTH with 2 and 3 times less memory usage and computational cost than the best scored approach.

1. Introduction

Future video prediction is a challenging task that recently received much attention due to its capabilities for learning in an unsupervised manner, making it possible to leverage large volumes of unlabelled data for video-related tasks such as action and gesture recognition, body pose recovery, and video segmentation. One of the main problems when approaching this task is the need of expensive models both in terms of memory and computational power in order to capture the variability present in video data. Another problem is the propagation of errors in recurrent models, which is tied to the inherent uncertainty of video prediction: given a series of previous frames, there are multiple feasible futures. This, left unchecked, results in a blurry prediction averaging the space of possible futures that propagates back into the network when predicting subsequent frames.

In this work we propose a new approach to recurrent auto-encoders (AE) with state sharing between encoder and decoder. We show how the exposed state in Gated Recurrent Units (GRU) can be used to create a bijective mapping between the input and output of each layer. Creating a stack of these layers allows for a bidirectional flow of information similar to an AE¹, but with many inherent advantages. This allows to reduce memory and computational costs during both training and testing: only the encoder or decoder needs to be executed for both input encoding and prediction,

¹Code available at <https://github.com/moliu@uoc/frnn>

respectively. Furthermore, the representation is stratified so that only part of the input needs to be encoded at each layer: low level information that is not necessary to capture higher level dynamics is not passed to the next layer. It naturally provides an identity mapping of the input as starting point, facilitating the initial stages of training. The approach also mitigates the propagation of errors: while it does not solve the problem of blur, it prevents its magnification in subsequent predictions. Furthermore, an already trained network can be deconstructed in order to analyse the role of each layer in the final predictions, making the model more explainable. Since the encoder and decoder states are shared, the architecture can be thought of as a recurrent auto-encoder folded in half, with corresponding encoder and decoder layers overlapping. We call our method Folded Recurrent Neural Network (fRNN). In summary, our list of contributions is as follows:

- A new shared-state recurrent AE with low memory and computational costs.
- Mitigation of error propagation through time.
- It naturally provides an identity function during training.
- Model explainability through layer removal.
- Model optimisation through layer removal.
- Demonstration of representation stratification.

The rest of the paper is organised as follows. Section 2 reviews related work. Section 3 presents the proposed method. Section 4 performs a quantitative and qualitative analysis of the method against state of the art alternatives. Finally, Section 5 concludes the paper.

2. Related work

Much research has been done on future video prediction in recent years. In this section we review main works, organising them into non-recurrent and recurrent models. We finish by highlighting the conceptual similarities between some of these approaches and the proposed method.

Non-recurrent approaches. Most non-recurrent techniques focus on solving problems related to the probability distribution of possible futures or the introduction of a priori information to guide the prediction into a more restricted output space. One of the first techniques tackling the problem of multiple possible futures was *Cross Convolutional Networks* (CCN) [18]. It predicts multiple possible future frames from a single image. The network generates a distribution of future motions based on the motion image between the last pair of frames and a multi-scale pyramid representing the last frame. A sampled frame motion is decoded into convolutional kernels and applied to the encoded pyramid of image frames to generate the future prediction.

Vondrick *et al.* [16] proposed a model based on convolutional adversarial networks to generate a video sequence

from a given single frame. They use a two stream network to model background and moving elements separately in static camera videos. Amersfoort *et al.* [14] developed a model to predict movement instead of working at pixel level. They extracted affine transformations between overlapping patches in consecutive frames to be fed into a CNN. Applying the predicted new transformation to the last frame in the sequence allowed to generate the next frame.

Vukotić *et al.* [17] use a convolutional AE taking a single frame along with a time differential which is fed after encoding frame information. The goal is to predict a single future frame at a given time interval from the input one. *Deep Voxel Flow* (DVF) [5] uses a convolutional AE network with unpooling layers in the decoder and skip connections between corresponding layers of the encoder and decoder. It feeds triplets of consecutive frames as input, predicting the next frame as output. During training, it uses an L1 reconstruction loss with Total Variation regularisation to minimise target image blur and enforce coherence.

Recurrent approaches. Given the sequential nature of future video prediction, recurrent approaches form the bulk of the scientific literature in the topic. Most works focus on the prediction blur and network capacity problems. Ranzato *et al.* [10] was one of the first recurrent proposals for frame prediction. They realised common losses introduced blur to the predictions and stressed the need for specialised ones. They adapted a RNN model from NLP to predict video sequences. They quantized image patches into a dictionary and reduced the generation problem to predicting the index in the dictionary for each image region of the next frame.

Mathieu *et al.* [7] proposed an AE multi-scale architecture to predict future frames. They used an adversarial setting and proposed the Gradient Difference Loss to promote sharp predictions. Oh *et al.* [8] predict future frames on Atari games conditioning on the action taken by the player, reducing the space of possible futures. It uses a convolutional AE, where the representation is transformed by an action-specific transform before decoding. They make two proposals for the last layer of the encoder: a regular fully-connected layer and a recurrent one, obtaining better results with the recurrent model. Patraucean *et al.* [9] combine a recurrent convolutional LSTM AE with optical flow. The approach predicts a flow map and uses it to wrap the previous frame. While this method is capable of learning long-range dependencies between frames, the use of optical flow to update the frame tends to introduce artefacts for large or complex motions. Srivastava *et al.* [13] also use a recurrent AE approach where an input sequence is encoded and its state is copied into the decoder. The decoder is then applied to generate a given number of frames. This model does not need to apply both the encoder and decoder at each time step, but is limited to a single recurrent layer for each part. Two versions of the model are proposed: a conditional ver-

sion taking the last generated frame as input to the decoder and an unconditioned version.

Brabandere & Jia *et al.* [4] developed the Dynamic Filter Network. This architecture uses a recurrent convolutional network to generate filters based on the input sequence. The filter is then applied to the last frame through another convolutional network in order to predict the next frame. Villegas *et al.* [15] propose a model treating motion and appearance separately. They use an autoencoder architecture where the encoder works separately for motion, using CNN + LSTM with difference images as input, and appearance, using a CNN with the last frame of the sequence as input. The decoder receives a concatenation of the encoded representations and multi-scale residual connections coming from each branch. *PredNet* [6] is a recurrent residual network using convolutional LSTM layers. It is temporally recurrent like previous methods, but also contains multiple recurrent blocks at the frame level, each minimising the discrepancies from the previous block prediction.

Convolutional Dynamic Neural Advection (CDNA) introduced skip connections to recurrent convolutional AEs [2]. It uses the AE to generate a series of affine transform maps and compositing masks. Then, it generates multiple images with each affine transform map and fuses them using the compositing masks. The goal is to predict a sequence of future frames from a physical system, based on both the previous frames and the state of a robotic arm interacting with the scene. Similarly, *Video Ladder Networks* (VLN) [1] proposed a convolutional AE topology with skip connections between corresponding levels of the encoder and decoder. Pairs of convolutions are grouped into residual blocks. The information is passed horizontally between corresponding blocks, both by directly passing the output to the decoder block and by using a recurrent bridge layer. This topology is further extended with *Recurrent Ladder Networks* (RLN) [3], where the recurrent bridge connections are removed, and the residual blocks replaced by recurrent layers. This results in recurrent layers taking three inputs: cell state, output of the previous layer, and output of the corresponding layer from the previous encoding/decoding step.

Both VLN and RLN share some similarities with our approach: they both propose a recurrent AE with bridge connections between encoder and decoder. This allows for representation stratification, reducing the capacity needs of the subsequent layers. However, using skip connections instead of state sharing has some disadvantages: higher number of parameters and memory requirements, impossibility to skip the encoding/decoding steps (resulting in a higher computational cost) and reduced explainability due to not allowing layers to be removed after training. Finally, bridge connections do not provide an initial identity function during training. This makes it hard for the model to converge in some cases: when the background is homogeneous the

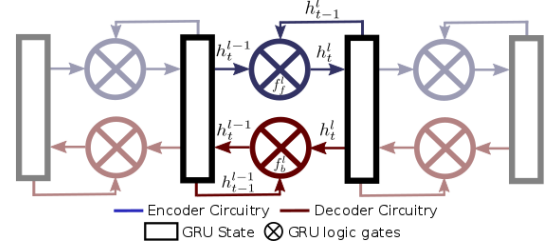


Figure 1. Scheme of a Bijective Gated Recurrent Unit. Blue and red correspond to forward and backward gates, respectively. Rectangles represent the recurrent state cell.

model may not learn a proper initial mapping between input and output, but set the weights to zero and adjust the bias of the last layer, eliminating the gradient in the process. We expand on and evaluate these differences throughout the following sections.

3. Proposed method

We propose an architecture based on recurrent convolutional AEs to deal with network capacity and error propagation problems on the future video prediction task. It consists on a series of bijective GRUs that allow for a bidirectional flow of information between states by providing an extra set of gates. These are then stacked, forming an encoder and decoder using the forward and backward functions of the bijective GRUs (Figures 1, 2). We call it Folded Recurrent Neural Network (fRNN). Because of the state sharing between encoder and decoder, this topology has several advantages: stratification of the encoded information, lower memory and computational requirements compared to regular recurrent AEs, constrained propagation of errors, and increased explainability through layer removal.

3.1. Bijective Gated Recurrent Units

GRUs have their state fully exposed to the output layer. This allows us to define a bidirectional mapping between input and output by replicating the logic gates of the GRU layer. Let's define the output of a GRU at layer l and time step t as $h_t^l = f_f^l(h_t^{l-1}, h_{t-1}^l)$ given an input h_t^{l-1} and its state at the previous time step h_{t-1}^l . A second set of weights can be used to define an inverse mapping $h_{t-1}^{l-1} = f_b^l(h_t^l, h_t^{l-1})$ using the output of the forward function at the current time step to update its input, which is treated as the hidden state of the inverse function. This is illustrated in Figure 1. We will refer to this double mapping as bijective GRU (bGRU).

3.2. Folded Recurrent Neural Network

By stacking multiple bGRUs, a recurrent AE is obtained. Given n bGRUs, the encoder is defined by the set of forward functions $E = \{f_f^1, \dots, f_f^n\}$ and the decoder by the set of backward functions $D = \{f_b^n, \dots, f_b^1\}$. This is illustrated in Figure 2, and is equivalent to a recurrent AE with shared states, with 3 main advantages: 1) It is not neces-

sary to feed the predictions back into the network in order to generate the following predictions. Because the states are shared, the decoder already updates all the states except for the bridge state between encoder and decoder. The bridge state is updated by applying the last layer of the encoder before generating the next prediction. The shadowed area in Figure 2 shows the section of the computational graph that is not required when performing multiple sequential predictions. For the same reason, when considering multiple sequential elements before prediction, only the encoder is required; 2) Because the network updates its states from the higher level representations to the lowest ones during prediction, errors introduced at a given layer during generation are not propagated back into deeper layers, leaving the higher-level dynamics unaffected; 3) The model implicitly provides a noisy identity model during training, as it is shown in Figure 8, when all bGRU layers are removed. The input state of the first bGRU layer is either the input image itself or, when first applying a series of convolutional layers, an over-complete representation of the input. A noise signal is introduced to the representation by the backward function of the untrained first bGRU layer. This provides the model with an initial identity model. As we show in Section 4.3, this helps the model to converge in some datasets like MMNIST: when the same background is shared across instances, it prevents the model from killing the gradients by adjusting the biases to match the background and setting the weights to zero.

This approach shares some similarities with VLN and RLN. As with them, part of the information can be passed directly between corresponding layers of the encoder and decoder, not having to encode a full representation of the input into the deepest layer. However, our model implicitly passes the information through the shared recurrent states, making bridge connections unnecessary. When compared against an equivalent recurrent AE with bridge connections, this results in a much lower computational and memory cost. More specifically, the number of weights in a pair of forward and backward functions is equal to $3(\overline{h^{l-1}}^2 + \overline{h^l}^2 + 2\overline{h^{l-1}} \overline{h^l})$ in the case of bGRU, where $\overline{h^l}$ corresponds to the state size of layer l . When establishing bridge connections as in the case of VLN and RLN, that value is increased to $3(\overline{h^{l-1}}^2 + \overline{h^l}^2 + 4\overline{h^{l-1}} \overline{h^l})$. This corresponds to an increase of 44% in the number of parameters when one state has double the size of the other, and of 50% when they have the same size. Furthermore, both the encoder and decoder must be applied at each time step. Overall, the memory usage is doubled and the computational cost increased by a factor of between 2.88 and 3.

3.3. Training Folded RNNs

In a regular recurrent AE, a ground truth frame is introduced at each time step by applying both encoder and

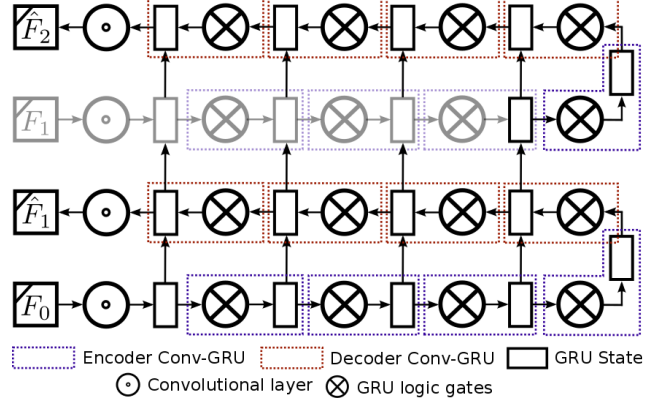


Figure 2. Folded Recurrent Neural Network topology. The recurrent states of the encoder and decoder are shared, resulting in a bidirectional mapping between states.

decoder. The output is used as a supervision point, comparing it to the next ground truth frame in the sequence. This implies all predictions are at a single time step from the last ground truth prediction. Here, we propose a training approach for Folded RNNs that exploits the ability of the topology of skipping the model encoder or decoder at a given time step. First g ground truth frames are shown to the network by passing them through the encoder. The decoder is then applied p times, producing p predictions. This approach results in only half the memory requirements: either encoder or decoder is applied at each step, never both. This has the same advantage as the approach by Srivastava [13], where recurrently applying the decoder without further ground truth inputs encourages the network to learn video dynamics. This also prevents the network from learning an identity model, that is, copying the last input to the output.

4. Experiments

We analyse our proposal on three public datasets and compare its performance against state of the art alternatives.

In Section 4.1 we introduce the considered data and evaluation protocol, and in Section 4.2 we present the methods used for comparison. Quantitative and qualitative analyses are presented in Sections 4.3 and 4.4, respectively. Finally, an analysis of the representation stratification of the proposed topology is performed in Section 4.5.

4.1. Data and evaluation protocol

We considered 3 datasets of different complexity in order to analyse the performance of the proposed method: Moving MNIST (MMNIST)[13], KTH [11], and UCF101 [12].

MMNIST consists of 64×64 greyscale sequences of length 20 displaying pairs of digits moving around the image. The sequences are generated by randomly sampling pairs of digits and trajectories. It contains a fixed test partition with 10000 sequences. We generated a million extra

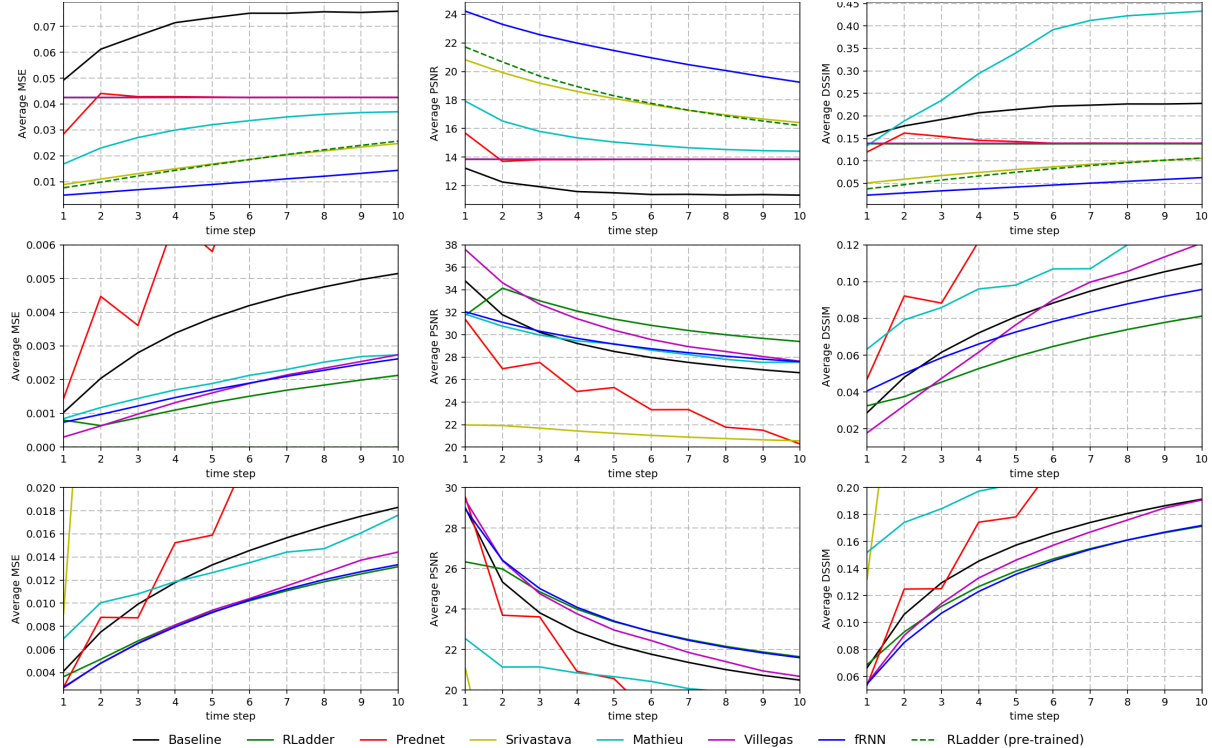


Figure 3. Quantitative results on the considered datasets in terms to the number of time steps since the last input frame. From top to bottom: MMNIST, KTH, and UCF101. From left to right: MSE, PSNR, and DSSIM.

	MMNIST			KTH			UCF101		
	MSE	PSNR	DSSIM	MSE	PSNR	DSSIM	MSE	PSNR	DSSIM
Baseline	0.06989	11.745	0.20718	0.00366	29.071	0.07900	0.01294	22.859	0.15043
RLadder	0.04254	13.857	0.13788	0.00139	31.268	0.05945	0.00918	23.558	0.13395
Prednet [6]	0.04137	14.017	0.14201	0.00807	24.635	0.13588	0.02124	20.398	0.19013
Srivastava [13]	0.01737	18.183	0.08164	0.00995	21.220	0.19860	0.14866	10.021	0.42555
Mathieu [7]	0.03071	15.361	0.32770	0.00194	29.097	0.10018	0.01287	20.492	0.20730
Villegas [15]	0.04254	13.857	0.13896	0.00165	30.946	0.07657	0.00940	23.457	0.14150
fRNN	0.00947	21.386	0.04376	0.00175	29.299	0.07251	0.00908	23.872	0.13055

Table 1. Average results over 10 time steps.

samples for training. KTH consists of 600 videos of 15-20 seconds from 25 subjects performing 6 actions in 4 different settings. The videos are all grayscale, at a resolution of 120×160 pixels and 25 fps. The dataset has been split into subjects 1 to 16 for training, and 17 to 25 for testing, resulting in 383 and 216 sequences, respectively. The frame size is reduced to 64×80 using bilinear interpolation, removing 5 pixels from the left and right borders before resising. UCF101 displays 101 actions, such as playing instruments, weight lifting or playing a wide range of sports. It is the most challenging dataset considered, showing a high intra-class variability. It contains 9950 training sequences and 3361 test sequences. Sequences are RGB at a resolution of 320×240 pixels and 25 fps. To increase motion between consecutive frames, one of every two frames was removed. As with KTH, the frame size is reduced to 64×85 .

All methods are tested using 10 input frames to generate the following 10 frames. We use 3 common metrics for video prediction analysis: Mean Squared Error (MSE),

Peak Signal-to-Noise Ratio (PSNR), and Structural Dissimilarity (DSSIM). MSE and PSNR are objective measurements of reconstruction quality. DSSIM is a measure of the perceived quality. For DSSIM we use a Gaussian sliding window of size 11×11 and $\sigma = 1.5$.

4.2. Methods

To train the proposed method we used RMSProp with learning rate of 0.0001 and batch size of 12, selecting a random sub-sequence at each epoch. Initial weights were set using orthogonal initialisation, with biases set to 0. For testing, all possible sub-sequences of length 20 were considered. Our network topology consists of two convolutional layers followed by 8 bijective GRU layers, applying a 2×2 max pooling every 2 layers. We use deconvolution and nearest neighbours interpolation to invert the convolutional and max pooling layers, respectively. We train with L1 loss.

We compare against the following methods: Prednet [6], Srivastava *et al.* [13], Mathieu *et al.* [7] and Villegas *et*

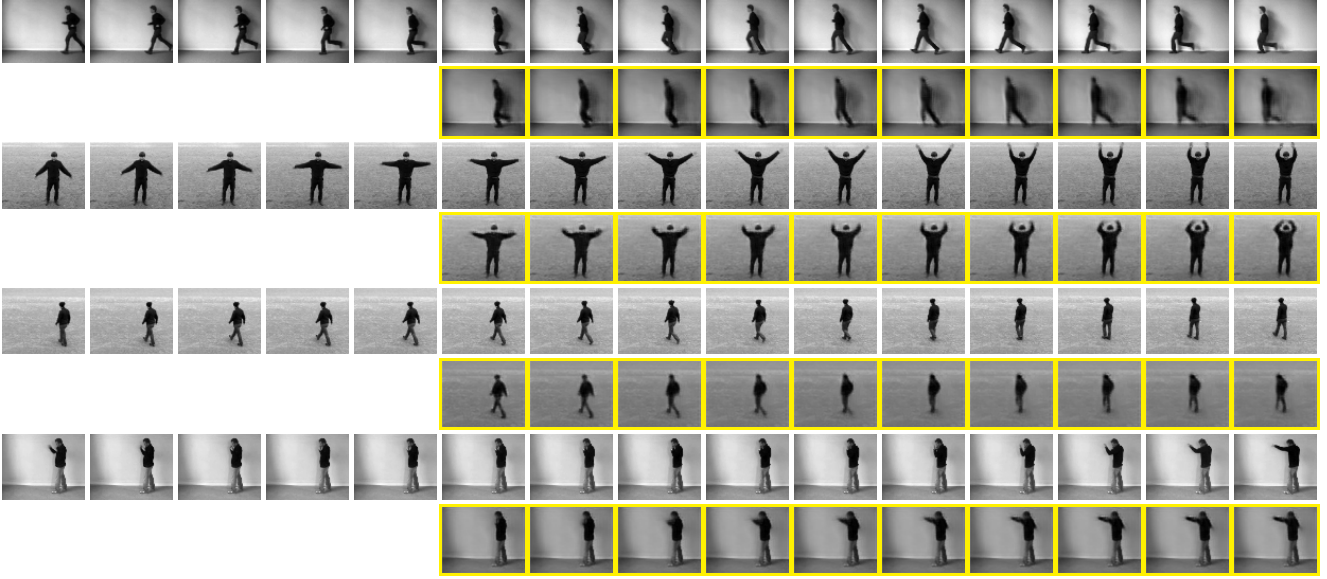


Figure 4. KTH fRNN predictions. First row for each sequence shows last 5 inputs and target frames. Yellow frames are model predictions.



Figure 5. MMNIST fRNN predictions. First row per sequence shows last 5 inputs and target frames. Yellow means prediction.

al. [15]. They are recurrent AEs, adapted for training on sequences of length 20. We used topologies and parameters defined by the authors. We also include a stub baseline model predicting the last input frame. We also design a second baseline (RLadder) to evaluate the advantages of using state sharing. RLadder has the same topology as the Folded RNN, but uses bridge connections between corresponding encoder and decoder layers. This is similar to how RLN [3] work, but using regular conv GRU layers in the decoder. Note that in order to keep the same state size on GRU layers, using bridge connections doubles the memory cost and almost triples the computational cost (Section 3.2).

4.3. Quantitative analysis

The first row of Figure 3 displays the results for the MMNIST dataset for the proposed method, baselines, and state of the art alternatives. The only methods to provide accurate predictions on this dataset are the fRNN models and the method by Srivastava *et al.*. Most other methods predict a black frame, with Mathieu *et al.* progressively blurring the digits. The problem with these methods is the loss of gra-

dient during the first stages of training. On more complex datasets the methods start by learning an identity function, then refining the results. This is possible since in many sequences most of the frames remains unchanged. In the case of MMNIST, where the background is homogeneous, it is much easier for the models to set the weights of the output layer to zero and set the biases to match the background colour. This cuts the gradient and prevents further learning. Srivastava *et al.* use an auxiliary decoder to reconstruct the input frames, forcing the model to learn an identity function. This, as discussed at the end of Section 3.2, is naturally done by our method, that in turn gives an initial solution to improve on, preventing the models from learning a black image. In order to verify this effect, we pre-trained RLadder on the KTH dataset. While this dataset has completely different dynamics, the initial step to solve the problem remains: providing an identity function. Afterwards the model is fine-tuned on the MMNIST dataset. As it is shown in Figure 3 (dashed lines), this results in the model converging, with an accuracy comparable to Srivastava for the 3 evaluation metrics. With most methods not converging, fRNN performs best on all time steps and metrics, followed by Srivastava *et al.* and the pre-trained RLadder. Mean scores are shown in Table 1.

On the KTH dataset, as shown in Table 1, the best approach is our RLadder baseline followed by fRNN and Villegas *et al.* [15], both having similar results, but with Villegas *et al.* having slightly lower MSE and higher PSNR, and fRNN a lower DSSIM. While both approaches obtain comparable average results, the error increases faster over time in the case of Villegas *et al.* (second row in Figure 3).

In the case of the UCF101 dataset, as shown in Table 1, our fRNN approach is the best performing method for all

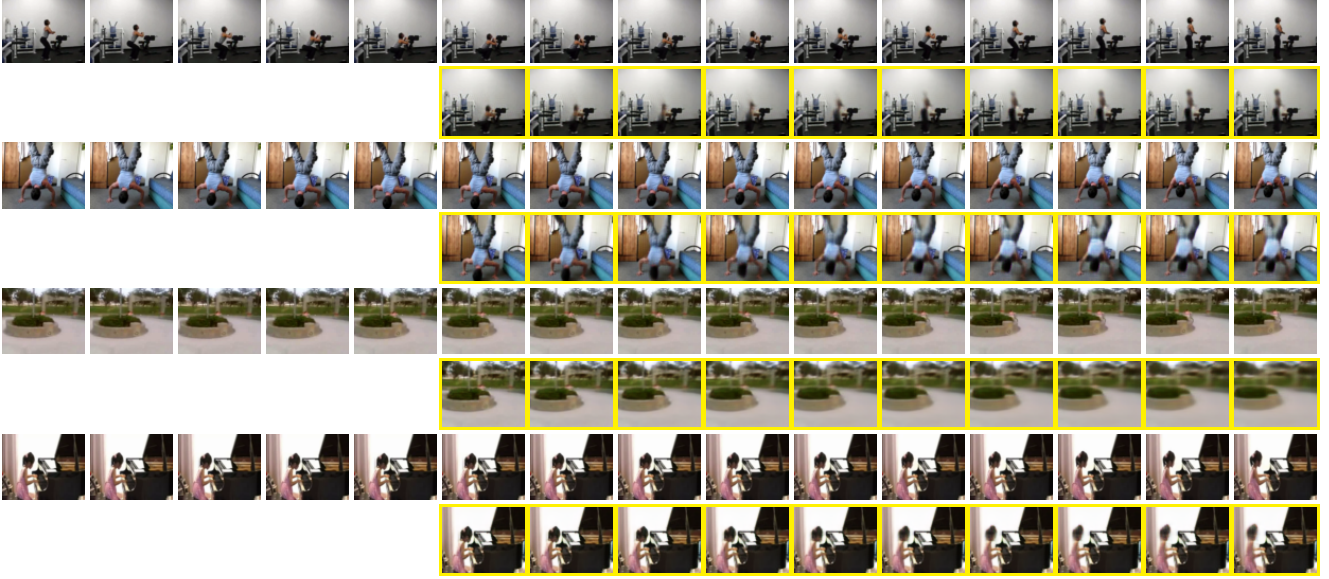


Figure 6. UCF fRNN predictions. First row for each sequence shows last 5 inputs and target frames. Yellow frames are model predictions.

3 metrics. When looking at the third row of Figure 6, one can see that Villegas *et al.* starts out with results similar to fRNN on the first frame, but as in the case of KTH and MMNIST, the predictions degrade faster than with the proposed approach. Two methods display low performance in most cases. Prednet works well for the first predicted frame in the case of KTH and UCF101, but the error rapidly increases on the following predictions. This is due to a magnification of artefacts introduced on the first prediction, making the method unable to predict multiple frames without supervision. In the case of Srivastava *et al.* the problem is about capacity: it uses fully connected LSTM layers, making the number of parameters explode quickly with the state cell size. This severely limits the representation capacity for complex datasets such as KTH and UCF101.

Overall, for the considered methods, the proposed fRNN is the best performing on MMNIST and UCF101, the later being the most complex of the 3 datasets. We achieved these results with a simple topology: apart from the proposed bGRU layers, we use conventional max pooling and layers with an L1 loss. There are no normalisation or regularisation mechanisms, specialised activation functions, complex topologies or image transform operators. In the case of MMNIST, fRNN shows the ability to find a good initial representation and converges to good predictions where most other methods fail. In the case of KTH, fRNN has an overall accuracy comparable to that of Villegas *et al.*, being more stable over time. It is only surpassed by the proposed RLadder baseline, a method equivalent to fRNN but with 2 and 3 times more memory and computational requirements.

4.4. Qualitative analysis

In this section we evaluate our approach qualitatively on some samples from the three considered datasets.

In this section we evaluate our approach qualitatively, observing how the model behaves in terms of predicting movement dynamics, reconstructing occluded regions and specially on the propagation of blur. We then compare predictions from our approach against those of other state of the art methods.

Figure 5 shows the last 5 input frames from some MMNIST sequences along with the next 10 ground truth frames and their corresponding fRNN predictions. The ten predictions are generated sequentially without showing the previous ground truth/prediction to the network, that is, only using the decoder. As it can be seen, the digits maintain their sharpness across the sequence of predictions. Also, the bounces at the edges of the image are done correctly, and the digits do not distort or deform when crossing. This shows the network internally encodes the appearance of each digit, making it possible to reconstruct them after sharing the same region in the image plane.

Qualitative examples of fRNN predictions on the KTH dataset are shown in Figure 4. It shows three actions: hand waving, walking, and boxing. The blur stops increasing after the first three predictions, generating plausible motions for the corresponding actions while background artefacts are not introduced. Although the movement patterns for each type of action have a wide range of variability on its trajectory, bGRU gives relatively sharp predictions for the limbs. The first and third examples also show the ability of the model to recover from blur. The blur slightly increases for the arms while the action is performed, but decreases again as these reach the final position.

Figure 6 shows fRNN prediction examples from the UCF101 dataset. These correspond to two different physical exercises and a girl playing the piano. One common attribute for all images is the static parts do not lose sharp-

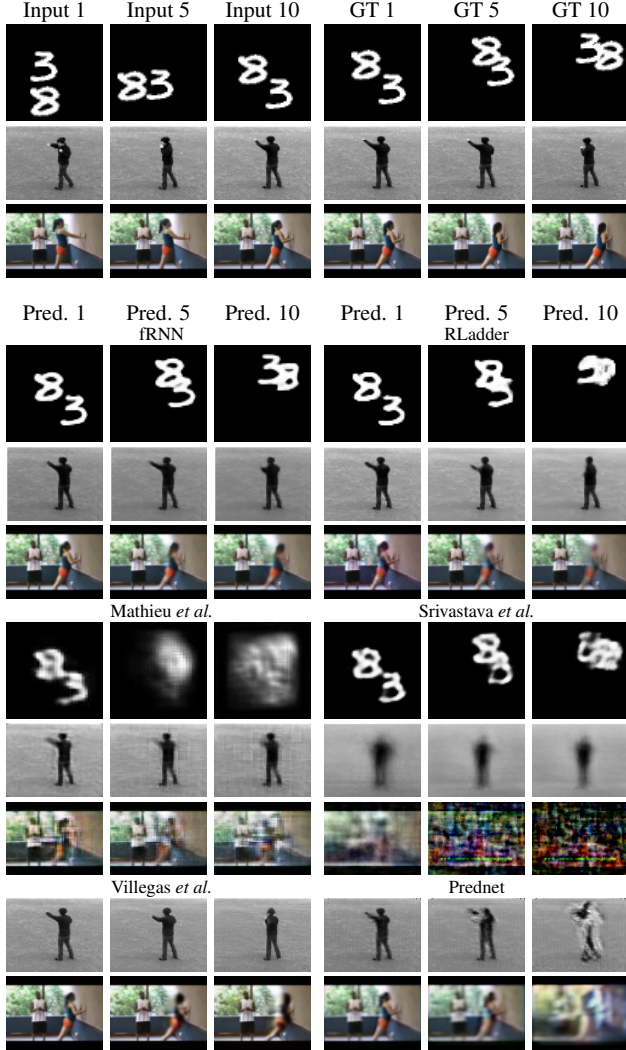


Figure 7. Predictions at 1, 5, and 10 time steps from the last ground truth frame. RLadder predictions on MMNIST are from the model pre-trained on KTH.

ness over time, and when occluded and later revealed, the background is properly reconstructed. As for dynamic regions, the network correctly predicts actions with low variability, as shown in rows 1-2, where a repetitive movement is performed, and in last row, where the girl moves back to a correct body posture. Regarding the introduction of blur, these dynamic regions introduce it due to the uncertainty of the action, averaging the possible futures.

The first row also shows an interesting behaviour: while the woman is standing up, the upper body becomes blurry due to uncertainty, but as the woman finishes her motion and ends up in the expected upright position, the frames sharpen again. Since the model does not propagate errors to deeper layers nor makes use of previous predictions for the following ones, the introduction of blur does not imply this blur will be propagated. In this example, while the middle motion could have multiple predictions depending

on the movement pace and the inclination of the body while performing it, the final body pose has a lower uncertainty.

In Figure 7 we compare predictions from the proposed approach against the RLadder baseline and other state of the art methods. For the MMNIST dataset we did not consider Villegas *et al.* and Prednet since these methods fail to successfully converge and they predict a sequence of black frames. From the rest of approaches, fRNN obtains the best predictions, with little blur or distortion. The RLadder baseline is the second best approach. It does not introduce blur, but heavily deforms the digits after they cross. Srivastava *et al.* and Mathieu *et al.* both accumulate blur over time, but while the former does so to a smaller degree, the later makes the digits unrecognisable after five frames.

For KTH, Villegas *et al.* obtains outstanding qualitative results. It predicts plausible dynamics and maintains the sharpness of both the individual and background. Both fRNN and RLadder follow closely, predicting plausible dynamics, but not being as good as Villegas *et al.* at maintaining the sharpness of the individual.

On UCF101 the best prediction is obtained by our model, with little blur or distortion compared to the other methods. The second best is Villegas *et al.*, successfully capturing the movement patterns but introducing more blur and important distortions on the last frame. When looking at the background, fRNN proposes a plausible initial estimation and progressively completes it as the woman moves. On the other hand, Villegas *et al.* modifies already generated regions as more background is uncovered, generating an unrealistic sequence regarding the background.

Srivastava and Prednet fail on both KTH and UCF101. Srivastava *et al.* heavily distort the frames. As discussed in Section 4.3, this is due to the use of fully connected recurrent layers, which constrains the state size and prevents the model from encoding relevant information on more complex scenarios. In the case of Prednet, it makes good predictions for the first frame, but rapidly accumulates artefacts.

4.5. Representation stratification analysis

In this section the stratification of the sequence representation among the bGRU layers is analysed. Because bGRU units allow for a bijective mapping between the states, it is possible to remove the bottom-most layers of an already trained network. This allows us to check how the predictions are affected, providing an insight on the dynamics captured by each layer. To the best of our knowledge, this is the first topology allowing for a direct observation of the behaviour encoded on each layer.

Specifically, the same sequences are predicted multiple times, removing a layer each time. This is shown in Figure 8 for the MMNIST dataset. The analysed model consists of 10 layers: 2 convolutional layers and 8 bGRU layers. Firstly, removing the last 2 bGRU layers has no sig-

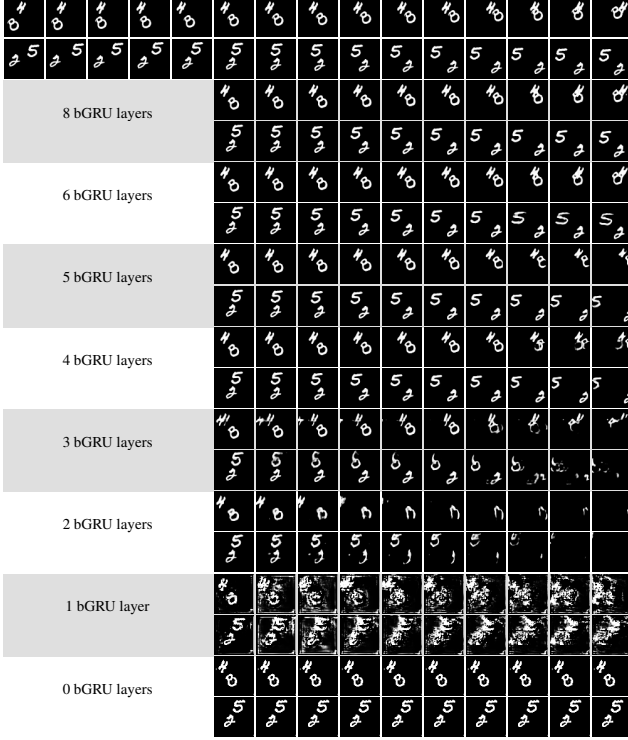


Figure 8. Moving MNIST predictions with fRNN layer removal.

nificant impact on prediction. This shows that, for this simple dataset, the network has a higher capacity than required. Further removing layers does not result in a loss of pixel-level information, but on a progressive loss of behaviours, from more complex to simpler ones. This means information at a given level of abstraction is not encoded into higher level layers. When removing the third deepest bGRU layer, the digits stop bouncing and keep their linear trajectories, exiting the image. This indicates this layer is in charge of encoding information on bouncing dynamics. When removing the next layer, digits stop behaving correctly on the boundaries of the image. Parts of the digit bounce while others keep the previous trajectory. While this also has to do with bouncing dynamics, the layer seems to be in charge of recognising digits as single units following the same movement pattern. When removed, different segments of the digit are allowed to move as separate elements. Finally, with only 3-2 bGRU layers the digits are distorted in various ways. With only two layers left, the general linear dynamics are still captured by the model. By leaving a single bGRU layer, the linear dynamics are lost.

According to these results, linear movement dynamics are captured at the pixel level on the first two bGRU layers. The next two start aggregating these movement patterns into single-trajectory components, preventing their distortion. Also the collision of these components with image bounds are detected. The fifth layer aggregates single-motion components into digits, forcing them to follow the same motion.

This seems to have the effect of preventing bounces, likely due to only one of the components reaching the edge of the image. It is the sixth bGRU layer that provides a coherent bouncing pattern for the whole digit.

5. Conclusions

We presented Folded Recurrent Neural Networks, a new recurrent architecture for video prediction with lower computational and memory cost compared to equivalent recurrent AE models. This is achieved by using the proposed bijective GRUs, which horizontally pass information between the encoder and decoder. This eliminates the need for using the entire AE at any given step: only the encoder or decoder needs to be executed for both input encoding and prediction, respectively. It also facilitates the convergence by naturally providing a noisy identity function during training. We evaluated our approach on three video datasets, outperforming state of the art prediction results on MMNIST and UCF101, and obtaining competitive results on KTH with 2 and 3 times less memory usage and computational cost than the best scored approach. Qualitatively, the model can limit and recover from blur by preventing its propagation from low to high level dynamics. We also demonstrated stratification of the representation, topology optimisation, and model explainability through layer removal. This is a straightforward process in this topology. Each layer has been shown to modify the state of the previous one by adding more complex behaviours: removing a layer eliminates its behaviours but leaves lower-level ones untouched.

References

- [1] F. Cricri, M. Honkala, X. Ni, E. Aksu, and M. Gabouj. Video ladder networks. *arXiv preprint arXiv:1612.01756*, 2016. [3](#)
- [2] C. Finn, I. Goodfellow, and S. Levine. Unsupervised learning for physical interaction through video prediction. In *Advances in Neural Information Processing Systems*, pages 64–72, 2016. [3](#)
- [3] A. Ilin, I. Prémont-Schwarz, T. H. Hao, A. Rasmus, R. Boney, and H. Valpola. Recurrent ladder networks. *arXiv preprint arXiv:1707.09219*, 2017. [3](#), [6](#)
- [4] X. Jia, B. De Brabandere, T. Tuytelaars, and L. V. Gool. Dynamic filter networks. In D. D. Lee, M. Sugiyama, U. V. Luxburg, I. Guyon, and R. Garnett, editors, *Advances in Neural Information Processing Systems 29*, pages 667–675. Curran Associates, Inc., 2016. [3](#)
- [5] Z. Liu, R. Yeh, X. Tang, Y. Liu, and A. Agarwala. Video frame synthesis using deep voxel flow. *arXiv preprint arXiv:1702.02463*, 2017. [2](#)

- [6] W. Lotter, G. Kreiman, and D. Cox. Deep predictive coding networks for video prediction and unsupervised learning. *arXiv preprint arXiv:1605.08104*, 2016. 3, 5
- [7] M. Mathieu, C. Couprie, and Y. LeCun. Deep multi-scale video prediction beyond mean square error. *arXiv preprint arXiv:1511.05440*, 2015. 2, 5
- [8] J. Oh, X. Guo, H. Lee, R. L. Lewis, and S. Singh. Action-conditional video prediction using deep networks in atari games. In *Advances in Neural Information Processing Systems*, pages 2863–2871, 2015. 2
- [9] V. Patraucean, A. Handa, and R. Cipolla. Spatio-temporal video autoencoder with differentiable memory. *arXiv preprint arXiv:1511.06309*, 2015. 2
- [10] M. Ranzato, A. Szlam, J. Bruna, M. Mathieu, R. Collobert, and S. Chopra. Video (language) modeling: a baseline for generative models of natural videos. *CoRR*, abs/1412.6604, 2014. 2
- [11] C. Schuldt, I. Laptev, and B. Caputo. Recognizing human actions: a local svm approach. In *Pattern Recognition, 2004. ICPR 2004. Proceedings of the 17th International Conference on*, volume 3, pages 32–36. IEEE, 2004. 4
- [12] K. Soomro, A. R. Zamir, and M. Shah. Ucf101: A dataset of 101 human actions classes from videos in the wild. *arXiv preprint arXiv:1212.0402*, 2012. 4
- [13] N. Srivastava, E. Mansimov, and R. Salakhudinov. Unsupervised learning of video representations using lstms. In *International Conference on Machine Learning*, pages 843–852, 2015. 2, 4, 5
- [14] J. R. van Amersfoort, A. Kannan, M. Ranzato, A. Szlam, D. Tran, and S. Chintala. Transformation-based models of video sequences. *CoRR*, abs/1701.08435, 2017. 2
- [15] R. Villegas, J. Yang, S. Hong, X. Lin, and H. Lee. Decomposing motion and content for natural video sequence prediction. *ICLR*, 1(2):7, 2017. 3, 5, 6
- [16] C. Vondrick, H. Pirsiavash, and A. Torralba. Generating videos with scene dynamics. In D. D. Lee, M. Sugiyama, U. V. Luxburg, I. Guyon, and R. Garnett, editors, *Advances in Neural Information Processing Systems 29*, pages 613–621. Curran Associates, Inc., 2016. 2
- [17] V. Vukotić, S.-L. Pinteá, C. Raymond, G. Gravier, and J. Van Gemert. One-step time-dependent future video frame prediction with a convolutional encoder-decoder neural network. *arXiv preprint arXiv:1702.04125*, 2017. 2
- [18] T. Xue, J. Wu, K. Bouman, and B. Freeman. Visual dynamics: Probabilistic future frame synthesis via cross convolutional networks. In *Advances in Neural Information Processing Systems*, pages 91–99, 2016. 2